Mid-infrared imaging of dust in galaxies

van der Wolk, Guido

4 The Spitzer [3.6]−[4.5] colour of active galactic nuclei

– G. van der Wolk, P.D. Barthel, and R.F. Peletier –
In preparation

We investigate the nature of galaxy nuclei with a strong near-infrared [3.6]−[4.5] colour excess. Such red nuclei are present in 3/24 of the early-type spiral Sa galaxies from the SAURON sample (NGC 2273, 4235 and 4293). We compare the *Spitzer* colours of the complete set of 24 Sa nuclei with a few well-known nearby active galactic nuclei (M 51, 81, 87 and 104) and present new colour maps. The nearby active nuclei also show a near-infrared excess in comparison to normal nuclei which are dominated by stellar and star formation emission. This gives rise to the interpretation that this excess is related to supermassive black hole accretion. The near-infrared emission of active nuclei can be explained as arising from either hot dust or a power-law spectral distribution. The sources with this excess all have compact radio cores with high brightness temperature. In comparison to other *Spitzer* studies it seems that 2-dimensional high resolution near-infrared imaging is a most efficient way of finding low-luminosity active galactic nuclei.

4.1 Introduction

It is now certain that almost all galaxies host supermassive black holes in their nuclei (Richstone et al. 1998), that these are often actively accreting matter (Ho 2008) and, most critically, that the mass of these central black holes scales with large-scale properties of the galaxy, such as the stellar velocity dispersion (Gebhardt et al. 2000; Ferrarese & Merritt 2000), and the mass of the bulge (Marconi & Hunt 2003). This fundamental connection between the central regions of a galaxy and its properties on much larger scales is thought to be a result of the supermassive black hole regulating the amount of accreting matter, and thus the rate of star formation, in its host system

throughout the period of galaxy evolution (Silk & Rees 1998; Hopkins et al. 2008).

Optical spectroscopic surveys of local galaxies reveal that the nuclear activity in nearby galaxies is generally weak and shows a dichotomy with Hubble type. Emission line ratio diagnostics show that two-thirds of early-type galaxies (E-Sb) and only about 15 % of late-type galaxies (Sc-Sd) host active nuclei (Palomar survey; Ho 2008). Summed over all Hubble types 40 % of the galaxies can be considered active. Among the active galactic nuclei (AGN), low-ionization narrow emission line region (LINER) dominated nuclei are more common (50 %) than those of transitional (25 %) and Seyfert-type (25 %) (Kauffmann et al. 2003; Hao et al. 2005). LINER and Seyfert AGN are again subdivided in type 1 and type 2 sources according to the presence of broad Hα emission lines. The low detection rate of sources with broad emission lines (20-25 %), the so-called type 1 sources, could indicate the presence of opaque dust around the broad line region (BLR), the region where these broad Hα lines originate, or else that this BLR is simply absent. Whereas a BLR is a clear manifestation of an accretion disk, narrow lines of low-ionization species could simply arise from circumnuclear star formation.

That accretion activity is less common in type 2 than type 1 sources can be deduced from high-resolution radio and X-ray studies. The presence of a compact radio core with high brightness temperature is a good AGN indicator since the radio emission is unrelated to star formation. Low brightness temperature radio emission could be related to supernova remnants or star-forming regions. Radio cores are detected in 44 % of the LINERs and 47 % of the Seyfert nuclei (Nagar et al. 2005). Type 2 sources of both LINER and Seyfert class have lower detection rates (30 %) than the type 1 sources (70 %). Transition objects sometimes (20 %) and H II nuclei almost never host a compact radio core (Filho et al. 2000). Although there is no complete X-ray survey of nearby galaxies the presence of a X-ray core is also a good AGN indicator. X-ray cores are found in 90 % of the Seyferts, 80 % of the LINERs and 70 % of the transition objects (Ho 2008). X-ray emission, however, can also have a stellar origin and the resolution of X-ray images is low.

These radio and X-ray core statistics seem to indicate the validity of a unification model for low-luminosity AGN in nearby galaxies based on accretion power (Ho 2008). Accretion rates determined from the X-ray core luminosities, as well as Hα emission line luminosity and radio core power, reveal a sequence of decreasing accretion rate going from Seyfert 1 to 2 to LINER 1 to 2 to transition objects. Type 1 sources show higher accretion rates than type 2 systems. At the lowest accretion rates the broad line region and torus disappear. The spectral energy distributions of low-luminosity AGN (LLAGN) suggest that the physics of these accretion discs is different from luminous AGN in radio galaxies and quasars. The absence of the big blue bump at optical-UV wavelengths and the presence of a mid-infrared bump suggest a three-component system with a puffed up radiative inefficient accretion flow (RIAF), a truncated thin disc and a nuclear jet (Rees et al. 1982; Chen & Halpern 1989; Halpern et al. 1996; Quataert 2003; Ho 2008).

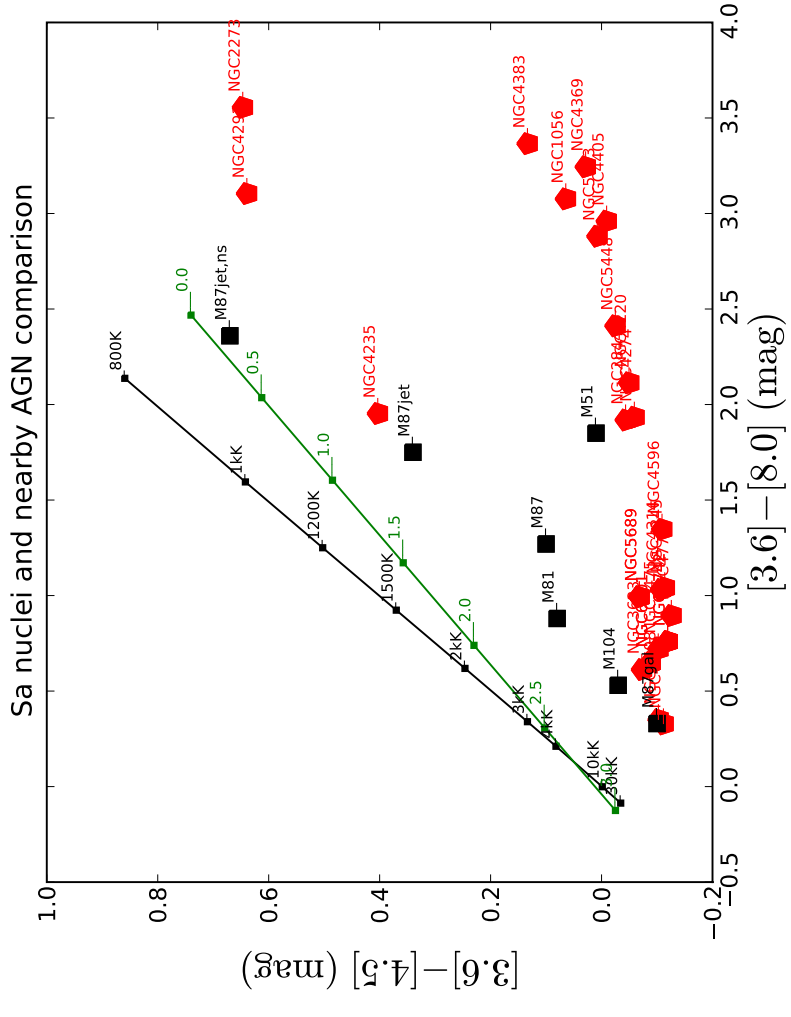

Figure 4.1: *Spitzer* colour-colour diagram. SAURON Sa sample nuclei are plotted in red and nearby active galaxy nuclei in black. For M 87 we also indicate the colours of the large-scale jet at knots A/B indicated as M87jet, the stellar emission at the same radius as the jet (M87gal) and the stellar-subtracted jet emission (M87jet,ns). Black bodies at various temperatures are plotted with a black line. Power-law models $\nu F_\nu \propto \nu^\alpha$ at various spectral indices $-1 \leq \alpha \leq 3$ are plotted with a green line.

At near-infrared wavelengths (2–5 μm) AGN also show prominent emission. A good tool to study AGN and their hosts are $JHKL$ (1–3.8 μm) colour diagrams, since stellar and non-stellar emission of galaxy nuclei have different locations in these diagrams (Glass & Moorwood 1985; Alonso-Herrero et al. 1998). The near-infrared emission of AGN is found to be either due to a power-law spectral distribution or due to hot dust (1 200 K). Dust of this temperature must be located very close to the AGN and is likely of graphite nature. Graphite grains have a high sublimation temperature, i.e. they can survive close to the AGN (Mor et al. 2009). Measuring over large 20 arcsec diameter apertures, Gallimore et al. (2010) show that reddened [3.6]−[4.5] colours are related to accretion power. The bumps as measured by [3.6]−[4.5] colour are generally present in Seyfert 1 galaxies and Seyfert 2 galaxies with hidden broad line regions detected via spectropolarimetry, and absent in Sy 2's with no proof for a hidden broad line region, LINERs and H II galaxies. In a comparison of radio galaxies and quasars Leipski et al. (2010) find that quasars do show a near-infrared bump while radio galaxies do not. This absence of the near-infrared bump in radio galaxies at high redshift is likely due to dust obscuration.

In Chapter 2 we have shown that 2 out of 5 of the SAURON early-type Sa galaxies optically classified as Seyfert and 1 out of 8 of the LINERs, and none of the non-AGN have clear near-infrared AGN signatures. The nuclei of these three galaxies (NGC 2273, 4235 and 4293) show a near-infrared [3.6]−[4.5] excess with colours > 0.3 mag in the magnitude system in a 2 arcsec diameter aperture. This is shown again in Fig. 4.1. In this Chapter we investigate the nature of this excess. We compare the near-infrared colours of the nuclei of our galaxies with those in nearby, well-known AGN in M 51, M 81, M 87 and M 104. To find out whether the near-infrared excess of the nuclei is an efficient way of finding AGN we compare our data with radio and X-ray core literature data.

4.2 The [3.6]–[4.5] colour of nearby AGN

To investigate whether the red [3.6]−[4.5] colours of the Sa nuclei are really related to AGN emission we examine a few nearby AGN in the galaxies Messier 51/NGC 5194, M 87/NGC 4486, M 81/NGC 3031, and Sombrero/M 104/NGC 4594. For M 81 we discuss literature data (Willner et al. 2004). For M 51, 87 and 104 we present flux and colour maps (Fig. 4.5, 4.6 and 4.7) constructed from IRAC and MIPS 24 μm archive data in a similar way as for the SAURON sample (Chapter 2). We choose these objects because the spectral energy distributions (SED) of these AGN are well-studied at many wavelengths, they have low activity and their host galaxies span the full range in Hubble type (Table 4.1). If the nuclei of these low-activity galaxies are similarly reddened in the [3.6]−[4.5] colour this would mean that the near-infrared excess is an efficient way of finding AGN.

The nucleus of Sab galaxy M 81 has been classified as of either LINER (Heckman 1980) or Seyfert 1.5 type (Ho et al. 1997a) and has a redder *Spitzer* colour than the rest of the galaxy (Willner et al. 2004) with a [3.6]−[4.5] central value of > 0.2 mag and a [3.6]−[4.5]$= 0.08$ mag colour in a 2 arcsec diameter aperture. This reddening is

Table 4.1: Properties of a few well-known nearby active galaxies

Source	AGN	Hubble	D	$\log(L_r)$	$\log(L_x)$	σ	$\log L_{bol}$
			Mpc	erg s^{-1}	erg s^{-1}	km s^{-1}	erg s^{-1}
(1)	(2)	(3)	(4)	(5)	(6)	(7)	(8)
NGC 3031 / M 81	S1.5	Sab	3.6	37.14	39.38	162	41.3
NGC 4486 / M 87	L2	E$^+$0	16.8	39.03	40.78	298	41.4
NGC 4594 / M 104	L2	Sa	9.2	37.90[a]	40.69	241	41.4
NGC 5194 / M 51	S2	Sbc	7.7	35.50[b]	41.03	96	42.2

Source	$\log M_{BH}$	$\frac{L_{bol}}{L_{Edd}}$	$\frac{[O\,III]}{H\beta}$	[3.6]−[4.5]	[3.6]−[8.0]	$\frac{[O\,IV]25.89}{[Ne\,II]12.81}$	$\frac{[Ne\,V]14.3}{[Ne\,II]12.81}$
	$M_\odot$			mag	mag		
(1)	(9)	(10)	(11)	(12)	(13)	(14)	(15)
NGC 3031	7.76	-4.54	0.61	0.08[c]	0.88[c]	0.17	<0.04
NGC 4486	8.83	-5.50	0.28	0.10	1.27	0.17	<0.02
NGC 4594	8.46	-5.13	0.20	−0.03	0.53	0.17	<0.03
NGC 5194	6.85	-2.72	0.95	0.01	1.85	0.43	0.07

Column (2) AGN type from Ho et al. (1997a), *Column (3)* Hubble type (RC3), *Column (4)* Distance, *Columns (5-6)* Logarithm of radio (15 GHz; Nagar et al. 2005, 5 GHz; Filho 2003 ([a]), 5 GHz; Crane & van der Hulst 1992 ([b])) and X-ray luminosity from Ho (2009), *Column (7)* central velocity dispersion, *Column (8)* Logarithm of bolometric luminosity from Ho (2009), *Column (9)* Logarithm of black hole mass calculated from the velocity dispersion σ using the $M_{BH} - \sigma$ correlation from Tremaine et al. (2002), *Column (10)* Logarithm of the Eddington ratio, *Column (11)* Logarithm of optical emission line ratios, *Columns (12-13) Spitzer* colours of nuclei measured from our maps or from Willner et al. (2004) ([c]), *Columns (14-15)* mid-infrared fine-structure line ratios from Pereira-Santaella et al. (2010).

likely unrelated to star formation, since the nucleus has a blue colour of [3.6]−[8.0]= 0.88 mag. The nucleus shows variability at optical wavelengths (Devereux et al. 2003) and in the 10 μm wavelength region (Grossan et al. 2001).

For the galaxies M 51, 87 and 104 we construct colour maps in a similar way as for the SAURON Sa sample (Chapter 2). The colour maps and photometry in apertures with diameters of 2 arcsec (Fig. 4.1) all reveal nuclei with reddened [3.6]−[4.5] colours. The elliptical galaxy M 87 with a nucleus that has been classified as of LINER 2 type (Ho et al. 1997a), has the reddest nucleus of these nearby AGN. M 87 is one of the nearest radio galaxies (Virgo A/3C 274) and is well-known for its highly collimated large-scale jet that is visible from radio to X-ray wavelengths. We also determine the IRAC colours of the jet knots A/B at 13 arcsec from the nucleus. To determine the non-thermal emission from the jet region we determine the stellar emission at a similar radius in the galaxy and subtract this stellar emission from the jet emission. The colours of the stellar emission (M87gal in Fig. 4.1) are around zero but slightly offset from a pure blackbody spectrum, due to CO absorption in the 4.5 micron band and dust heating from evolved stars. We find similar colours for the jet knots as seen through a screen of stellar emission (M87jet in Fig 4.1) as Shi et al. (2007). From our comparison with power-law models we see that this jet emission corresponds to power-law emission with a spectral index $\alpha \sim 1$, with $\nu F_\nu \propto \nu^\alpha$. Note that in this convention for α, the Rayleigh-Jeans tail of a blackbody spectrum would give $\alpha = 3$. The spectral index of the power-law stellar-subtracted jet emission (M87jet,ns in Fig. 4.1) indicate a flatter power-law with $\alpha = 0.3$. This is similar to what is found

from stellar-substracted images throughout the radio to 24 micron (Shi et al. 2007) and radio to optical range (Stiavelli et al. 1997; Shi et al. 2007).

The IRAC core emission of M 87 (Fig. 4.1) could indicate either a non-thermal or thermal component. Either way the component does not contribute a lot to the near-infrared nuclear emission, since its IRAC colours correspond to a steep spectral index ($\alpha \sim 2$) or a low fraction of hot dust (1 200 K). Unfortunately, it is difficult to determine the stellar emission contribution to the core using two-dimensional imaging. At longer wavelengths the stellar contribution is smaller. Considering the 5.8, 8.0 and 24 μm broadband emission of the non-stellar subtracted core in a 3 arcsec diameter aperture, we find a spectral index of $\alpha \sim 1$. With a *Spitzer*-IRS stellar spectra subtraction method, Buson et al. (2009) find that the stellar-subtracted spectrum of the core of M 87, within a 8 arcsec diameter aperture, has a power-law slope $\alpha = 0.19$ in the 5-20 μm range. This indicates a non-thermal origin for the near-infrared excess and is in line with ground-based high-resolution (0.5 arcsec) N-band (12 μm) nuclear values of Whysong & Antonucci (2004) and Perlman et al. (2007), who find that circumnuclear dust contributes little or nothing to the central mid-infrared emission in M 87. We note with interest that this behaviour is entirely conform our conclusion of Chapter 5, given the identification of Virgo A as radio galaxy of FR-I type.

The non-thermal or dust torus contribution to the core of the Sa galaxy M 104, classified as of LINER 2 type (Ho et al. 1997a), is small but nonzero since it is clearly offset from stellar emission in Fig. 4.1. Bendo et al. (2006) find a redder colour [3.6]−[4.5]= 0.14 mag than we do, but similar [3.6]−[8.0]= 0.62 mag colour for the nucleus from fitting the images with model components and conclude the emission must be related to a hot dust component around an AGN. The Sbc galaxy M 51, classified as of Seyfert 2 type (Ho et al. 1997a), is the only galaxy for which the nuclear colours in Fig. 4.1 indicate very little evidence for the presence of an AGN.

4.3 The nature of the near-infrared excess.

The *Spitzer* IRAC colour-colour diagram shows that nearby low-activity AGN and jet emission are offset from stellar or star formation emission in the [3.6]−[4.5] colour. The offset is similar to the three SAURON Sa galaxies but has lower magnitude. A similar offset is seen in JHKL (1–3.8 μm) colour-colour diagrams in $H-K$ and $K-L$ colours (Glass & Moorwood 1985; Alonso-Herrero et al. 1998). These diagrams indicate that the origin of this emission must be either a hot dust (1 200 K) or a power-law spectral distribution component.

From Fig. 4.1 we see that whatever the origin of these components, they are less prominent in the nearby low-activity AGN than in 3/24 galaxies in the SAURON Sa sample. The colours of NGC 4235 match well with those of the M 87 jet emission, and might thus be non-thermal radiation. On the other hand NGC 4235 has a much lower radio core flux (5 mJy at 5 GHz; Edelson 1987) than M 87, and Peletier et al. (1999) find that NGC 4235 has a rather flat J−H colour profile and an excess at the nucleus in a H−K colour profile. This and the location in the IRAC *Spitzer* colour diagram rather indicate a hot dust 1 200 K component. If the near-infrared radiation from NGC 2273

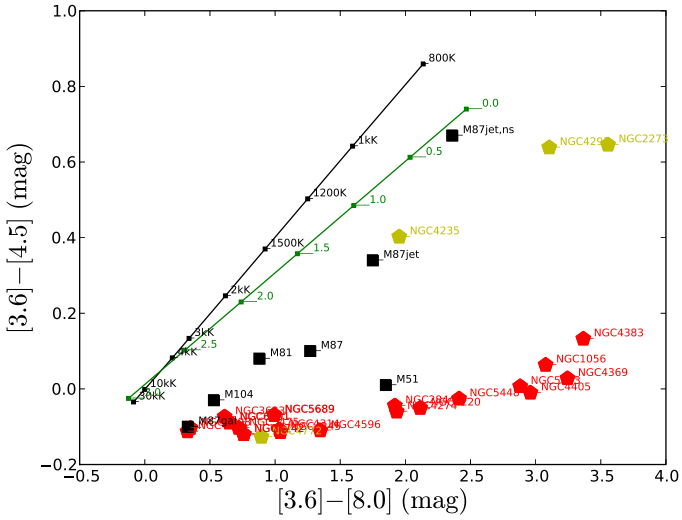

Figure 4.2: *Spitzer* colour-colour diagram. SAURON Sa sample nuclei with detected radio cores (Edelson 1987; Nagar et al. 2005) are plotted in yellow. Nearby AGN are plotted in black. See also the caption of Fig. 4.1.

and 4293 has a thermal origin their location in the *Spitzer* colour-colour diagram makes clear that this dust temperature must be below 800 K. Another explanation might be that these two galaxies host circumnuclear star formation alongside a hot dust component. In the next section we discuss the radio and X-ray properties of these active and inactive galaxies to find out whether a near-infrared excess is an efficient way of finding AGN.

4.4 A new detection method?

We compare the near-infrared AGN excess detected in the [3.6]–[4.5] colour maps of the SAURON Sa galaxy sample and the nearby AGN sample with the radio and X-ray AGN classification of these galaxies. Does our method only detect the most active AGN?

Radio cores

The presence of a compact radio core seems a good AGN indicator since the radio emission is unrelated to star formation. Radio cores with high brightness temperatures are detected in 44 % of the LINERs and 47 % of the Seyfert nuclei (Nagar et al. 2005). Type 2 sources of both LINER and Seyfert class have lower detection rates (30 %) than the type 1 sources (70 %). In our Sa sample there are 3 galaxies with compact (< 0.15 arcsec) radio cores as found with the 15 GHz VLA imaging survey of optically

classified AGN in the Palomar sample (Nagar et al. 2005): NGC 2273, 4293 and 4772. This radio survey includes 7 more of our Sa galaxies, and for which no radio core has been detected: NGC 3623, 4220, 4314, 4596, 4698, 5448, and 7742. The galaxy NGC 4235 has radio core emission at 5.0 GHz at 1.5 arcsec resolution, and has a flat radio spectrum (Edelson 1987). For the rest of the sample we checked whether they are detected in the 5 arcsec resolution 1.4 GHz FIRST survey of galaxies (White et al. 1997; Becker et al. 2003). We refer to radio core luminosities determined from these FIRST fluxes as upper limits. The data are listed in Table 4.2.

From the *Spitzer* colour-colour diagram we see that all our infrared-identified AGN have radio cores, i.e. the three uppermost yellow symbols in Fig. 4.2. Furthermore, the galaxy NGC 4772 has a radio core but no red [3.6]−[4.5] counterpart. It is possible that the activity restarted recently, and that a surrounding dust structure has not yet formed or is not yet heated. The radio core emission of this galaxy with a classical bulge (Chapter 3) might also be related to supernova remnants or starbursts. The brightness temperature has a lower limit of $\log(T_{\rm B}) > 6.8$ K (Nagar et al. 2005), which makes an AGN classification quite plausible. The three Sa galaxies do have lower radio core luminosities than the nearby AGN sample, while they have redder infrared colours, suggesting that the radio-to-infrared spectra are steeper for our Sa galaxies. This argues for a larger thermal component in the Sa galaxies. We have found high-resolution radio maps of NGC 2273, 4235 and 4293 but not for 4772. These maps show the presence of small-scale jets near the nuclei. NGC 2273 has a double jet (Nagar et al. 2005) and a small diffuse radio emission component alongside with it, which could be due to an outflow of gas from the nucleus (Mundell et al. 2009). NGC 4235 hosts two kilo-parsec scale radio lobes (Gallimore et al. 2006). The radio emission around the core in NGC 4293 is rather amorphous and hints at a thermal origin (Filho et al. 2006). The fact that this galaxy has the steepest radio-infrared spectral index could support a thermal origin as well.

X-ray cores

Although there is no complete X-ray survey of nearby galaxies, the presence of X-ray cores seems to be a better AGN indicator than the presence of radio cores. X-ray cores have a higher detection rate in optically classified AGN than radio cores (Ho 2008). X-ray cores are found in 90 % of the Seyferts and 80 % of the LINERs and 70 % of the transition objects. X-ray emission is also a good measure of bolometric AGN luminosity independent of dust obscuration. In the literature we find detections for 8 galaxies from our Sa sample with 2–10 keV X-ray luminosities (Ho 2009) acquired with a range in telescopes and resolutions (1–5 arcsec). Our infrared-identified AGN have the highest X-ray luminosities ($L_{\rm x} > 10^{40}$ erg s^{-1}; Table 4.2), although NGC 4293 has an upper limit to its luminosity. NGC 4772, with a radio core and no near-infrared excess, also has a fairly high X-ray luminosity, comparable to that of M 81. M 81 is the only galaxy of the nearby AGN sample with weak X-ray emission.

The galaxy NGC 7742, which has an optical classification as of transition or LINER 2 type, also has a high X-ray luminosity. This emission is probably related to stellar emission rather than to an AGN, since this galaxy has a massive

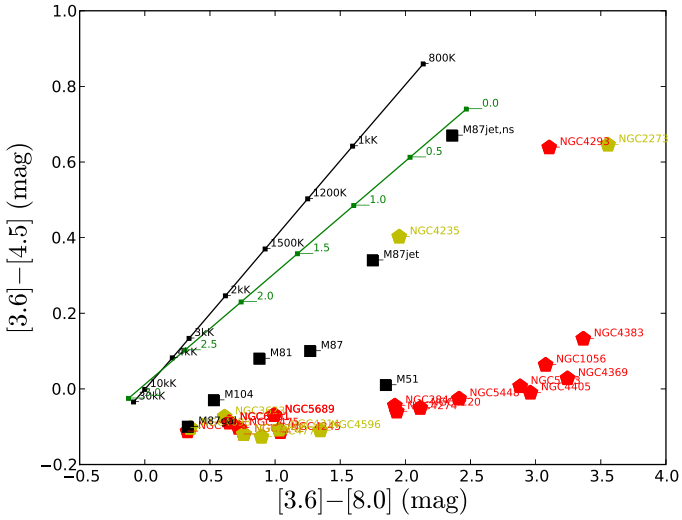

Figure 4.3: *Spitzer* colour-colour diagram. SAURON Sa sample nuclei with detected X-ray cores are plotted in yellow. Nearby AGN are plotted in black. See also the caption of Fig. 4.1.

bulge (Chapter 3). In Fig. 4.3 we indicate which of the galaxies have detected X-ray cores in the *Spitzer* colour-colour diagram. Remarkably, the AGN without a hot core and with X-ray emission are predominantly galaxies without much star formation ($[3.6]-[8.0] < 1.5$ mag). This could confirm that X-ray emission is related with evolved star emission in these galaxies. If we translate the X-ray emission to bolometric luminosities and Eddington ratios we find that all sources with X-ray detections and without near-infrared excess have Eddington ratios of $\log(L_{\rm bol}/L_{\rm Edd}) < -5.5$. It shows that our infrared detection method does not work anymore for such low Eddington ratios, and that the nuclear X-ray emission in such galaxies is most probably related to stellar and not to AGN emission.

4.5 Discussion

We find a good correspondence between the presence of a near-infrared excess and the presence of a compact high brightness temperature radio core ($L_{\rm r} > 10^{35}$ erg s^{-1}; < 0.15 arcsec), indicative of an AGN, in the nuclei of our SAURON Sa galaxies and nearby AGN sample. Of the 4 galaxies with a radio core 3 have a near-infrared excess. The nature of this emission can be attributed either to a non-thermal power-law spectral distribution or a hot dust component. NGC 4235 has a similar colour as the jet plus stellar emission in M 87 which could indicate the presence of considerable non-thermal emission, but has a rather weak radio core flux. In the nearby AGN sample and NGC 4235 a hot dust component temperature could be of the order

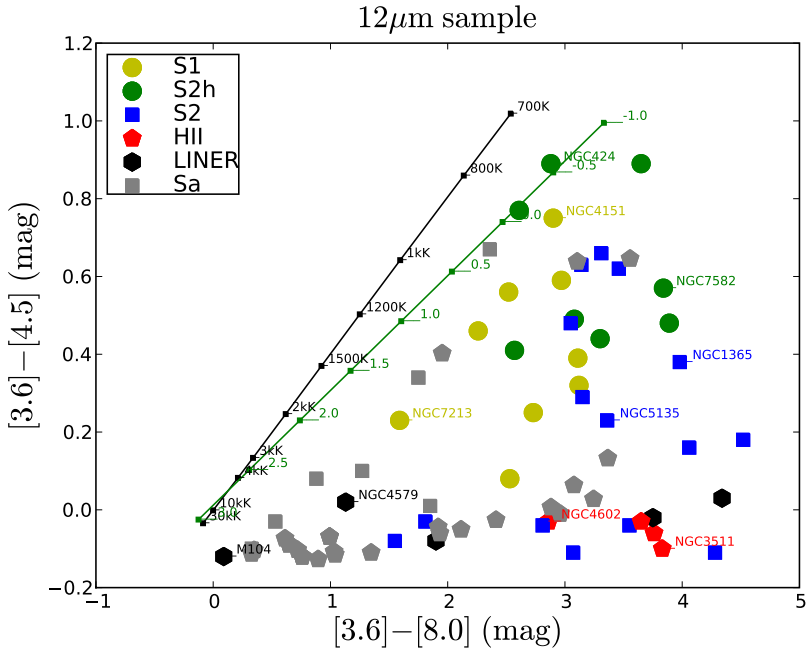

Figure 4.4: *Spitzer* colour-colour diagram for a subset of galaxies from the 12 μm sample. The colours are determined from 20 arcsec diameter photometry (Gallimore et al. 2010) and only galaxies at distances < 50 Mpc are included. Yellow symbols indicate Seyfert 1 galaxies, in green and blue Seyfert 2 galaxies with and without hidden broad line regions, in red galaxies with H II nuclei and in black LINER galaxies. In grey the nearby AGN and the SAURON Sa sample as in Fig. 4.1.

of 1 200 K, while in NGC 2273 and 4293 the component must have a temperature lower than 800 K. These temperatures could be slightly lower if circumnuclear star formation plays an additional role.

In Fig. 4.4 we compare our 2 arcsec diameter photometry of the SAURON Sa and nearby AGN sample with that of 20 arcsec diameter photometry of a subset of the 12 μm sample of active galaxies as determined by Gallimore et al. (2010). This sample includes Seyfert 1 galaxies, Seyfert 2 galaxies with and without hidden broad line regions, LINER galaxies and H II nuclei. This is a subselection of the full Gallimore et al. (2010) sample, limited to galaxies at distances < 50 Mpc. It shows that in the larger aperture the AGN in M 104 is not detected. However, one other LINER (NGC 4579) does show a near-infrared excess. Interestingly, this galaxy has a strong radio core (28 mJy at 15 GHz; Nagar et al. 2005). The colours of galaxies with H II nuclei NGC 3511 and 4602 are consistent with the star formation colours of the Sa nuclei, although NGC 3511 is quite blue in the [3.6]−[4.5] colour.

The colours of the Seyfert 1 galaxies NGC 7213 and 4151 and the Seyfert 2 galaxy with a hidden broad line region NGC 424 are probably not much affected by the larger aperture. If the near-infrared excess in NGC 424 and 4151 is due to a hot

dust component it is clear from this large aperture study that the dust temperature of these components must be lower than 800 K. Half of the Seyfert 1 and most of the Seyfert 2 galaxies are however a mixed bag (e.g. NGC 1365, 5135 and 7582) and are possibly affected by star formation from the host galaxy. Our study indicates that it would be fruitful to study in detail the colours of the nuclei of these galaxies using 2-dimensional near-infrared *Spitzer* imaging. In this way one can find out if circumnuclear star formation plays a role in Seyfert galaxies and get a better grip on the hot dust component temperature.

4.6 Summary and conclusions

We have investigated the nature of galaxy nuclei with a near-infrared $[3.6]-[4.5]$ colour excess of > 0.3 mag within a 2 arcsec diameter aperture. Such red nuclei are present in 3/24 of the early-type spiral Sa galaxies from the SAURON sample (NGC 2273, 4235 and 4293). We have compared the *Spitzer* colours of the 24 Sa nuclei with a few well-known nearby active galactic nuclei (M 51, 81, 87 and 104). The nearby active nuclei also show a near-infrared excess in comparison to normal nuclei which are dominated by stellar and star formation emission. This gives rise to the interpretation that this excess is related to supermassive black hole accretion.

The near-infrared emission of active nuclei can be explained as arising from either hot dust or a non-thermal power-law spectral distribution. NGC 4235 has a similar colour as the jet plus stellar emission in M 87 which could indicate considerable non-thermal emission, but has a rather weak radio core flux. For the nearby AGN sample and NGC 4235 a hot dust component temperature could be of the order of 1 200 K, while for NGC 2273 and 4293 the component must have a temperature lower than 800 K.

The sources with this near-infrared excess all have compact radio cores with high brightness temperature. However, one galaxy with such a radio core (NGC 4772) does not host a hot core. Possibly, the activity in the core has restarted recently. In comparison to other *Spitzer* studies it seems that 2-dimensional high resolution near-infrared imaging is a most efficient way of finding low-luminosity active galactic nuclei.

Appendix: Literature data and colour maps

The SAURON Sa sample

NGC 1056 — This galaxy is classified in the NASA extragalactic database (NED) as a Seyfert 2. The nucleus has a low [O III]/Hβ emission line ratio indicating star formation (Fig. 3.4). The mid-infrared fine structure lines indicate LINER activity (Tommasin et al. 2010).

NGC 2273 — This galaxy is classified as a Seyfert 2 (Ho et al. 1997a) and has a high [O III]/Hβ emission line ratio (Fig. 3.4) and a mid-infrared fine structure line ratio of [O IV]25.89/[Ne II]12.81 = 0.33 (Pereira-Santaella et al. 2010) consistent with an AGN classification.

NGC 4235 — This nearly edge-on galaxy is of Seyfert 1.2 type (Ho et al. 1997a). The high [O III]/Hβ emission line ratio confirms this (Fig. 3.4). The galaxy also has a strong mid-infrared fine structure line ratio of [O IV]25.89/[Ne II]12.81 = 0.87 (Pereira-Santaella et al. 2010).

NGC 4293 — This is a relatively highly inclined galaxy with a LINER type nucleus (Ho et al. 1997a). It has a strong dust lane passing close to the nucleus (Falcón-Barroso et al. 2006).

NGC 5953 — This galaxy is classified in NED as of Seyfert 2 type. The galaxy has a strong mid-infrared fine structure line ratio of [O IV]25.89/[Ne II]12.81 = 0.33 consistent with a Seyfert classification.

Table 4.2: Nuclear properties of the SAURON Sa sample

Source	AGN	$\log(L_r)$ (erg s^{-1})	$\log(L_x)$ (erg s^{-1})	σ km s^{-1}	$\log M_{BH}$ ($M_\odot$)	$\log L_{bol}$ (erg s^{-1})	$\log \frac{L_{bol}}{L_{Edd}}$	$\frac{[O\,IV]25.89}{[Ne\,II]12.81}$	$\frac{[Ne\,V]14.3}{[Ne\,II]12.81}$
(1)	(2)	(3)	(4)	(5)	(6)	(7)	(8)	(9)	(10)
NGC 1056	Sy2			83.62	6.61			0.12[a]	<0.05[a]
NGC 2273	Sy2	36.48	40.02	113.64	7.14	41.22	-4.02	0.35	0.11
NGC 2844	HII			97.99	6.88				
NGC 3623	L2::	<35.40	38.25	143.63	7.55	39.45	-6.20		
NGC 4220	T2	<35.79		100.36	6.93				
NGC 4235	Sy1.2	35.78[b]	42.25	151.41	7.64	43.45	-2.30	0.87	< 0.11
NGC 4245	HII			89.14	6.72				
NGC 4274	HII	<34.72[c]		103.73	6.98				
NGC 4293	L2	35.73	<39.37	104	6.99	<40.57	<-4.52		
NGC 4314	L2	<35.61	38.13	117.06	7.19	39.33	-5.97		
NGC 4369	HII	<34.97[c]		60.83	6.05				
NGC 4383	HII	<35.34[c]		102.86	6.97				
NGC 4405	HII			47.59	5.62				
NGC 4425				78.1	6.49				
NGC 4596	L2::	<35.63	38.65	140.14	7.51	39.85	-5.76		
NGC 4698	Sy2	<35.58	38.69	132.2	7.41	39.89	-5.62		
NGC 4772	L1.9	36.12	39.30	135.1	7.45	40.5	-5.05		
NGC 5448	L2	<36.08		120.31	7.24				
NGC 5475		<35.57[c]		94.4	6.82				
NGC 5689				153.97	7.67				
NGC 5953	Sy2	<36.08[c]		100.27	6.92			0.33	0.03
NGC 6501	L2::			224.19	8.33				
NGC 7742	T2/L2	<35.77	39.94	222.52	8.32	41.14	-5.28		

Column (2) AGN type from Ho et al. (1997a), *Columns (3-4)* Logarithm of 15 GHz radio (Nagar et al. 2005), 5 GHz radio (Edelson 1987), or 1.4 GHz radio (FIRST; Becker et al. 2003 ([c])) and X-ray luminosity (Ho 2009), *Column (5)* central velocity dispersion (Chapter 3), *Columns (6)* Logarithm of black hole mass calculated from the velocity dispersion σ using the $M_{BH} - \sigma$ correlation from Tremaine et al. (2002), *Column (7)* Logarithm of bolometric luminosity calculated from X-ray luminosity, *Column (8)* Eddington ratio, *Columns (9-10)* mid-infrared fine-structure line ratios from Pereira-Santaella et al. (2010) and Tommasin et al. (2010) ([a]).

Nearby AGN sample

M 81/NGC 3031 — The Sab galaxy M 81/NGC 3031 is one of the nearest spiral galaxies and hosts a LINER (Heckman 1980) or a Seyfert 1.5 nucleus (Ho et al. 1997a), a broad Hα emission line, a weak UV bump (Ho 2008), a radio core with a parsec-scale jet (Nagar et al. 2005), and a low-luminosity X-ray core (Ho 2009). The nucleus shows stronger dust heating than the disc (Bendo et al. 2010) at far-infrared wavelengths, 70, 160 and 250 μm, as detected with Herschel. Both the bolometric luminosity and black hole mass of this galaxy are quite low, yielding a low Eddington ratio of $\log(L_{\rm bol}/L_{\rm Edd}) = -4.5$. The mid-infrared fine structure line ratios [O IV]25.89/[Ne II]12.81 = 0.17 and [Ne V]14.3/[Ne II]12.81 < 0.02 of M 81 (Pereira-Santaella et al. 2010) indicate LINER rather than Seyfert activity.

M 87/NGC 4486 — The elliptical galaxy M 87/NGC 4486 is one of the nearest radio galaxies (Virgo A) and is well-known for its highly collimated large-scale jet that is visible from radio to X-ray wavelengths. From optical spectroscopy, the nucleus is classified as of LINER 2 type (Ho et al. 1997a). The infrared *Spitzer* spectrum does not show [Ne V]14.3 high-excitation lines, which confirms the LINER classification (Perlman et al. 2007; Pereira-Santaella et al. 2010).

M 104/NGC 4594 — The AGN in the Sa galaxy M 104/NGC 4594/Sombrero galaxy is also of LINER 2 type (Ho et al. 1997a). This nucleus lacks both a broad line region and dust torus (Ho 2008) and is weak but variable in the UV and has a variable radio (Filho 2003) and X-ray core (Ho 2009). The *Spitzer* IRS spectrum does not show the high-excitation [Ne V] line at 14.3 μm (Pereira-Santaella et al. 2010).

M 51/NGC 5194 — The AGN in the Sbc galaxy M 51/NGC 5194 is of Seyfert 2 type (Ho et al. 1997a). The AGN has a bright X-ray luminosity (Ho 2009), shows a high-excitation [Ne V] line at 14.3 μ and [O IV] line at 25.89 μm (Goulding & Alexander 2009) and a very weak radio core (Crane & van der Hulst 1992). The Eddington ratio of this galaxy is also the highest, $\log(L_{\rm bol}/L_{\rm Edd}) = -2.7$, of all four nearby AGN we discuss here. However, for this galaxy we calculate the bolometric luminosity from a X-ray 2-10 keV luminosity with a bolometric correction factor of $C_X = 15.8$ (Ho 2009), rather than from the SED as in M 81, M 87 and M 104. On the other hand the bolometric luminosities of these three galaxies do scale with their X-ray luminosities.

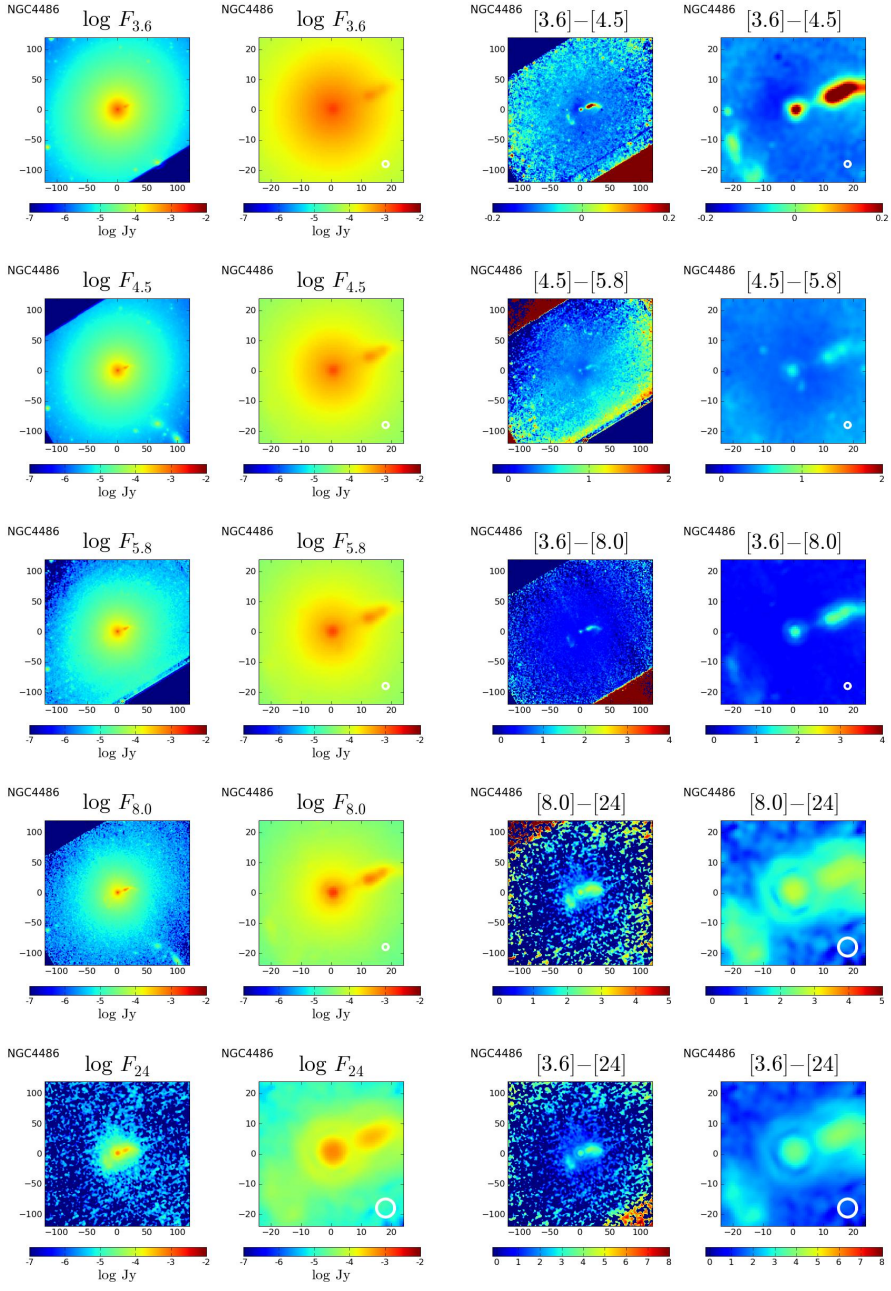

Figure 4.5: NGC 4486/M 87. North is up and East is left. The first and second column show the broadband *Spitzer* IRAC and MIPS flux maps on logarithmic scale in units of Jy/arcsec^2, 4 by 4 arcminutes in size, and the central 48 by 48 arcsecond. The third and fourth column show *Spitzer* colour maps in magnitudes on large scale and zoomed in.

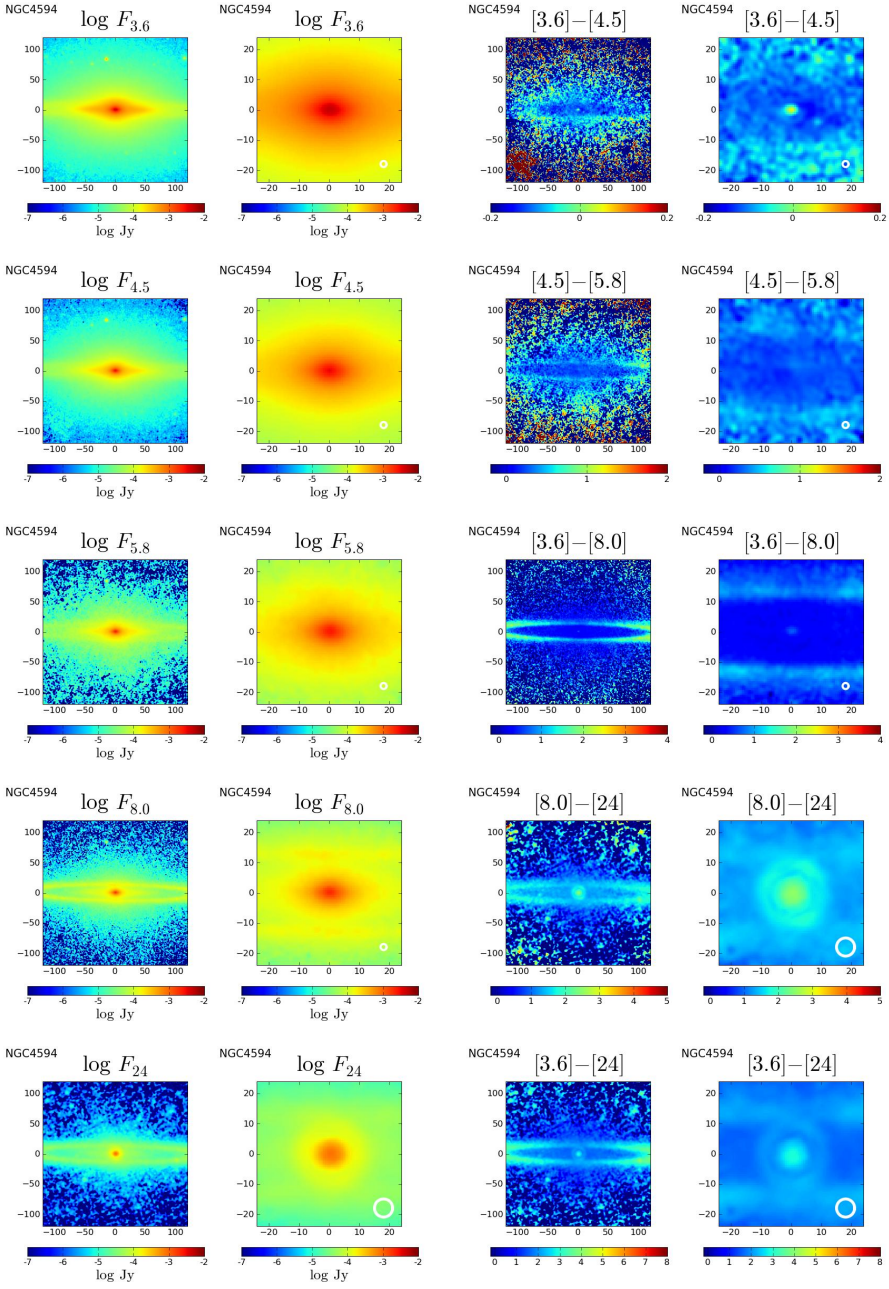

Figure 4.6: NGC 4594/M 104. See caption of Fig. 4.5.

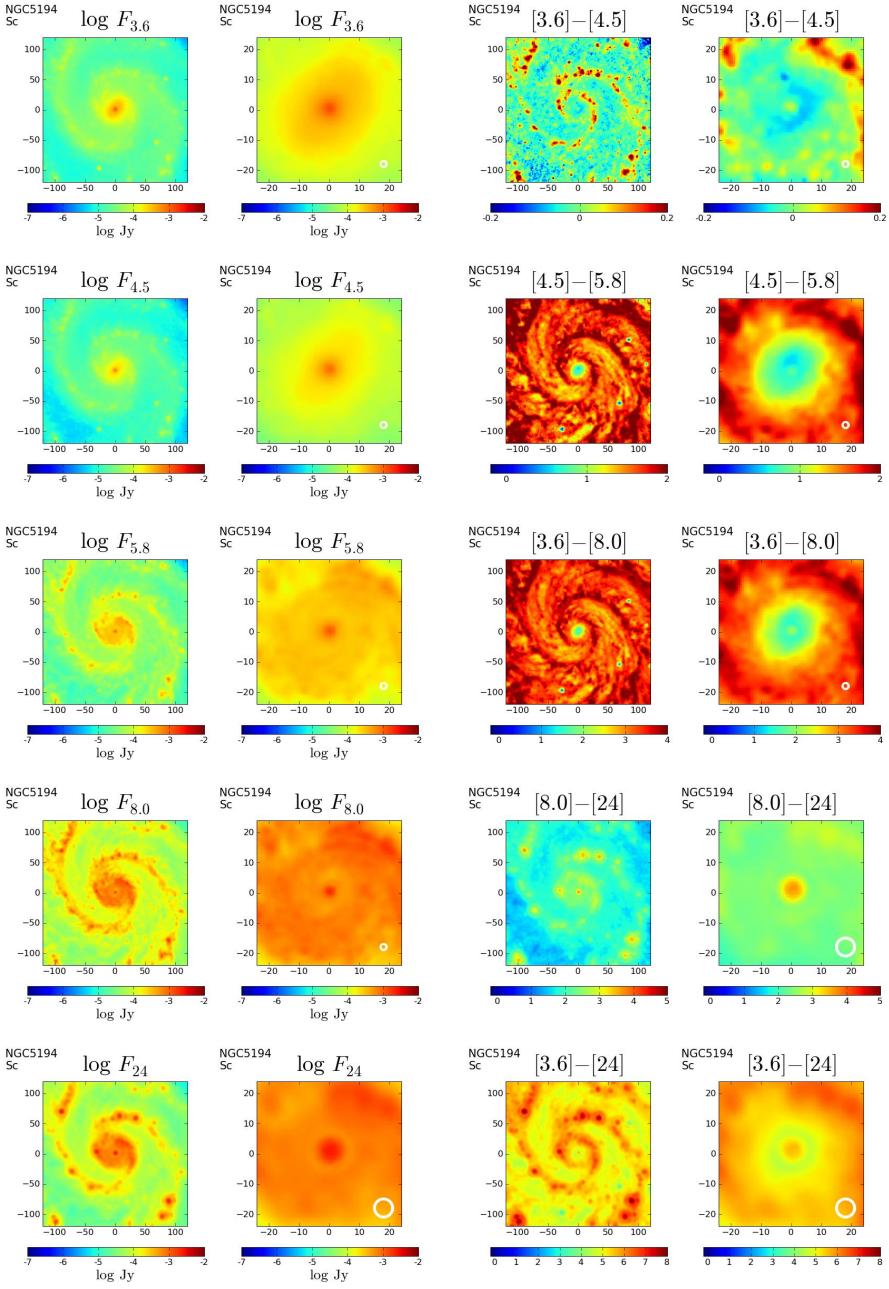

Figure 4.7: NGC 5194/M 51. See caption of Fig. 4.5.